J Braz. Soc. Mech. Sci. Eng. (2015) 37:325–337
DOI 10.1007/s40430-014-0183-6

TECHNICAL PAPER

Deformation and stress analysis of sandwich cylindrical shells with a flexible core using harmonic differential quadrature method

H. Shokrollahi · M. H. Kargarnovin · F. Fallah

Received: 14 January 2014 / Accepted: 16 April 2014 / Published online: 6 May 2014
© The Brazilian Society of Mechanical Sciences and Engineering 2014

Abstract In this paper, based on the high-order theory (HOT) of sandwich structures, the response of sandwich cylindrical shells with flexible core and any sort of boundary conditions under a general distributed static loading is investigated. The faces and the core are made of isotropic materials. The faces are modeled as thin cylindrical shells obeying the Kirchhoff–Love assumptions. For the core material, it is assumed to be thick and the in-plane stresses are negligible. The governing equations are derived using the principle of the stationary potential energy. Using harmonic differential quadrature method (HDQM), the equations are solved for deformation components. The obtained results are compared with finite element results for different sandwich shell configurations. Then, the effects of changing different parameters on the stress and displacement components of sandwich cylindrical shells are investigated. A comparison between HOT-HDQM and finite element results is presented for different sandwich shell configurations.

Keywords Sandwich cylindrical shells · Harmonic differential quadrature method · Flexible core · High-order theory · General lateral loading

1 Introduction

Sandwich shells are widely used in many engineering applications, especially in aerospace and marine industries. They commonly consist of two load carrying faces connected by usually soft inner layer (core). The faces are made of materials with high stiffnesses, as steel, aluminum alloys, reinforced plastics and the core can be made of corrugated sheet, wood, foam, rubber, etc. Generally, the sandwich shells are lightweight structures with very high stiffness to weight and strength to weight ratios and they also have very good thermal and acoustic isolation properties.

To date the study on the shell behavior is well developed and historically is back-dated to early 1940s. A summary of early works can be found in some textbooks written by Plantema [1], Allen [2], and Zenkert [3]. Some newer comprehensive reviews can be found in [4–7] in which various analytical and computational models for sandwich structures are presented. In overview of these works, it can be concluded that when the overall or global response of a sandwich shell is under consideration, there is no need to use complicated or high-order theories (HOTs). That is an accurate prediction of the shell response can be achieved using the classical sandwich shell theory assumptions. For a rather complicated case, for example study of the local buckling, wrinkling of the sandwich shells or in sandwich shells with more flexible cores, a high-order theory (HOT) of sandwich structures is required to reach better predictions. The HOT is developed by Frostig and coworkers [8–12] and either is challenged or implemented by many other researches in the last two decades. Generally, in most HOTs some prior assumptions are made with respect to the displacement field in the core. However, there are few HOTs that the displacements and the stresses of the core are determined through a 3D elasticity solution, see [13–16].

Generalized differential quadrature method (GDQM) is a rather new numerical method which has been widely used in solving problems in different engineering fields. The

H. Shokrollahi · M. H. Kargarnovin · F. Fallah (✉)
School of Mechanical Engineering, Sharif University of Technology, P.O. Box 14588-89694, Tehran, Iran
e-mail: fallah@sharif.ir

GDQM was developed by Shu and coworkers [18, 19] based on the DQ technique [20]. On the other hand, the harmonic differential quadrature method (HDQM) is a fast converging version of the GDQM [17]. In general, in all different versions of the DQ method, the partial derivative of a function, with respect to a spatial variable at a given discrete point, will be approximated by a linear summation of weighted function values at all discrete points chosen in the solution domain of the spatial variable [18, 19]. Some advantages of the DQ method in comparison with the finite element method (FEM) are the ease of its implementation on the governing equations and spending less computational efforts in solving any problem. The reason lies in the fact that in the DQ method the natural and essential boundary conditions must be satisfied simultaneously, while in FEM the natural boundary conditions are included in the weak form solution of the governing equations, and the approximate displacement functions must satisfy only the essential boundary conditions of the problem. In other words, the DQM and FEM deal with strong and weak forms of governing differential equations, respectively.

There are some works in the literatures in which the DQM has been used in static analysis of the laminated cylindrical shell panel. For example, Maleki et al. [21] used GDQM in static and transient analysis of thin/moderately thick laminated shell panels subjected to different loadings and boundary conditions. Tornabene et al. [22] applied the GDQM in the static analysis of laminated composite shell panel of revolution with various lamination schemes and different layers. Malekzadeh [23] used the DQM in the in-plane static analysis of laminated composite arches with any type of boundary conditions.

To the best knowledge of the authors, no work related to the static analysis of the sandwich cylindrical shell panels with general type of boundary conditions and subjected to any arbitrary lateral loading is reported in the literature. Only for the case of fully simply supported sandwich shells, an exact closed-form solution is presented using Fourier series [14]. In addition, to the best knowledge of the authors, there is no reported study in the open literature in which any version of the DQ methods is employed on the sandwich cylindrical shell panels.

The aim of the present work is to study the behavior of cylindrical sandwich shells with flexible core and any sort of boundary conditions under a generally distributed static loading using HDQM. The obtained results are compared with finite element results. Then, the effects of different parameters, including core flexibility, the core to the face thickness ratio and the ratio of shell curvature to thickness, on the stress and displacement components of sandwich cylindrical shells are investigated.

2 Problem definition and assumptions

Figure 1 shows an open sandwich cylindrical shell with general boundary conditions subjected to arbitrary lateral loadings (as a function of x and θ) imposed simultaneously at inner and outer surfaces. It is assumed that the loads are exerted in a rather quasi-static manner. The displacement components corresponding to the x (longitudinal), θ (circumferential) and z (radial) directions are represented by u, v and w, respectively. According to Fig. 1, β represents the subtended angle, R is the radii of curvature, L is the length of the shell, and h is the thickness. The sub/super scripts of t, c, and b denote the top face, the core, and the bottom face, respectively. Following main assumptions are considered;

- The faces and the core are assumed to be made of isotropic materials.
- Small deformation theory is considered for the analysis of elastic deformations.
- The faces are modeled as thin cylindrical shells and analyzed based on the classical Love's shell theory.
- The core is assumed to be thick and its thickness is much greater than the thicknesses of faces [i.e., (h_t, h_b) « h_c].
- The core and the faces are perfectly bonded that is no delamination will occur in the core/face interfaces.
- The core consists of a weak low density material compared to the faces, thus the in-plane stresses in the core, i.e., σ_x, σ_θ, and $\tau_{x\theta}$, are assumed to be negligible [13–16]. Based on these assumptions and HOT, the displacements and the stresses in the core are determined through a 3D elasticity solution.

3 Formulation

3.1 Strain displacement relations

Based on the classical shell theory, the displacement field components u, v, and w of an arbitrary point located in the domain of the faces are assumed as follows [24] (see Fig. 1):

$$u_i(x,\theta,z_i) = u_{0i}(x,\theta) - z_i \frac{\partial w_{0i}(x,\theta)}{\partial x}$$

$$v_i(x,\theta,z_i) = v_{0i}(x,\theta) - \frac{z_i}{R_i}\left(\frac{\partial w_{0i}(x,\theta)}{\partial \theta} - v_{0i}(x,\theta)\right); \quad i = t,b$$

$$w_i(x,\theta,z_i) = w_{0i}(x,\theta) \tag{1}$$

where u_{0i}, v_{0i} and w_{0i} are the displacements of a point located on mid-surface of the faces in x, θ and z directions, respectively. Based on HOT, there are no assumptions on the displacement field of the core, and the displacement components of an arbitrary point located on the core are

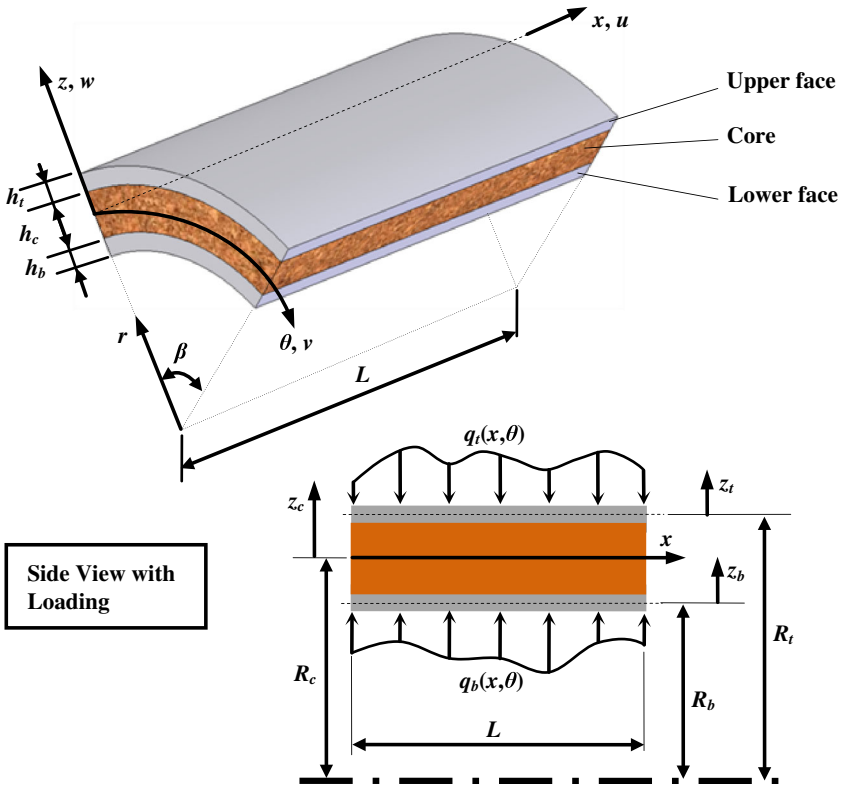

Fig. 1 Geometry of the sandwich cylindrical shell and applied loading

defined as $u_c(x, \theta, z_c)$, $v_c(x, \theta, z_c)$ and $w_c(x, \theta, z_c)$ and will be determined through a 3D elasticity solution.

Based on Eq. (1) and Kirchhoff–Love shell theory, the strain components in the upper and lower faces of the considered shell are as follows [25]:

$$\varepsilon_x^i = \frac{\partial u_{0i}(x,\theta)}{\partial x} - z_i \frac{\partial^2 w_{0i}(x,\theta)}{\partial x^2}$$

$$\varepsilon_\theta^i = \frac{1}{R_i}\frac{\partial v_{0i}(x,\theta)}{\partial \theta} + \frac{w_{0i}(x,\theta)}{R_i} + \frac{z_i}{R_i^2}\left(\frac{\partial v_{0i}(x,\theta)}{\partial \theta} - \frac{\partial^2 w_{0i}(x,\theta)}{\partial \theta^2}\right); \quad i = t, b$$

$$\gamma_{x\theta}^i = \frac{\partial v_{0i}(x,\theta)}{\partial x} + \frac{1}{R_i}\frac{\partial u_{0i}(x,\theta)}{\partial \theta} + \frac{z_i}{R_i}\left(\frac{\partial v_{0i}(x,\theta)}{\partial x} - 2\frac{\partial^2 w_{0i}(x,\theta)}{\partial x \partial \theta}\right) \tag{2}$$

Also, the kinematic relations used for the core are as follows:

$$\varepsilon_z^c = \frac{\partial w_c(x,\theta,z_c)}{\partial z}$$

$$\gamma_{xz}^c = \frac{\partial w_c(x,\theta,z_c)}{\partial x} + \frac{\partial u_c(x,\theta,z_c)}{\partial z}$$

$$\gamma_{\theta z}^c = \frac{\partial v_c(x,\theta,z_c)}{\partial z} + \frac{1}{R_c + z_c}\left(\frac{\partial w_c(x,\theta,z_c)}{\partial \theta} - v_c(x,\theta,z_c)\right) \tag{3}$$

Assuming perfect bond between the two faces and the core, the continuity conditions of interface displacements of the top and bottom interfaces are as follows:

$$u_c\left(x,\theta,\frac{h_c}{2}\right) = u_{0t}(x,\theta) + \frac{h_t}{2}\frac{\partial w_{0t}(x,\theta)}{\partial x} \tag{4a}$$

$$v_c\left(x,\theta,\frac{h_c}{2}\right) = v_{0t}(x,\theta) + \frac{h_t}{2R_t}\left(\frac{\partial w_{0t}(x,\theta)}{\partial \theta} - v_{0t}(x,\theta)\right) \tag{4b}$$

$$w_c\left(x,\theta,\frac{h_c}{2}\right) = w_{0t}(x,\theta) \tag{4c}$$

$$u_c\left(x,\theta,-\frac{h_c}{2}\right) = u_{0b}(x,\theta) - \frac{h_b}{2}\frac{\partial w_{0b}(x,\theta)}{\partial x} \tag{5a}$$

$$v_c\left(x,\theta,-\frac{h_c}{2}\right) = v_{0b}(x,\theta) - \frac{h_b}{2R_b}\left(\frac{\partial w_{0b}(x,\theta)}{\partial \theta} - v_{0b}(x,\theta)\right) \tag{5b}$$

$$w_c\left(x,\theta,-\frac{h_c}{2}\right) = w_{0b}(x,\theta) \tag{5c}$$

3.2 Stress–strain relations

Both faces and core isotropic materials will undergo an elastic deformation. For an isotropic material in the linear elastic range, the relation between in-plane stresses and

strains (in the two faces) and out-plane stresses and strains (in the core) is as follows:

$$\sigma_x^i = \frac{E^i}{1-v_i^2}\left(\varepsilon_x^i + v_i\varepsilon_\theta^i\right) = C_{11}^i\varepsilon_x^i + C_{12}^i\varepsilon_\theta^i$$

$$\sigma_\theta^i = \frac{E^i}{1-v_i^2}\left(\varepsilon_\theta^i + v_i\varepsilon_x^i\right) = C_{12}^i\varepsilon_x^i + C_{22}^i\varepsilon_\theta^i; \quad i = t, b$$

$$\tau_{x\theta}^i = \frac{E^i}{2(1+v_i)}\gamma_{x\theta}^i = C_{33}^i\gamma_{x\theta}^i \tag{6}$$

and.

$$\sigma_z^c = E_c\varepsilon_z^c$$

$$\tau_{iz}^c = G_c\gamma_{iz}^c;\ i = x, \theta \tag{7}$$

where E^i and υ_i, $i = t$, $b$are, the Young's modulus and Poisson's ratio of the top and bottom faces and E_c and G_c are, respectively, the Young's modulus and shear modulus of the core.

4 Governing equations and solution procedure

To obtain the governing differential equations, the principle of minimum total potential energy is employed [26]:

$$\delta\Pi = \delta(U - W) = 0 \tag{8}$$

where Π, U, and W are the total potential energy, strain energy, and the work done by the external loadings, respectively.

The strain energy of the considered shell is the summation of strain energy of each part, that is, top and bottom faces and the core section as:

$$U = U_t + U_c + U_b \tag{9}$$

Moreover, the variation of strain energy can be expressed in terms of stress and strain components as [26],

$$\begin{aligned}\delta U = &\int_{V_t}\left(\sigma_x^t\delta\varepsilon_x^t + \sigma_\theta^t\delta\varepsilon_\theta^t + \tau_{x\theta}^t\delta\gamma_{x\theta}^t\right)\mathrm{d}V_t \\ &+\frac{1}{2}\int_{V_c}\left(\sigma_z^c\delta\varepsilon_z^c + \tau_{xz}^c\delta\gamma_{xz}^c + \tau_{\theta z}^c\delta\gamma_{\theta z}^c\right)\mathrm{d}V_c \\ &+\frac{1}{2}\int_{V_b}\left(\sigma_x^b\delta\varepsilon_x^b + \sigma_\theta^b\delta\varepsilon_\theta^b + \tau_{x\theta}^b\delta\gamma_{x\theta}^b\right)\mathrm{d}V_b\end{aligned} \tag{10}$$

Also the variation of the work done by the external loads is:

$$\begin{aligned}\delta W = &\int_0^\beta\int_0^L q_t(x,\theta)\delta w_{0t}(x,\theta)R_t\mathrm{d}x\mathrm{d}\theta \\ &+\int_0^\beta\int_0^L q_b(x,\theta)\delta w_{0b}(x,\theta)R_b\mathrm{d}x\mathrm{d}\theta\end{aligned} \tag{11}$$

where $q_t(x, \theta)$ and $q_b(x, \theta)$ are the applied loads on the inner and outer surfaces of the shell.

Upon substitution of Eqs. 2 and 3 into 10, three sets of equations including the equilibrium equations and boundary conditions for the two faces and the core are obtained which are presented and discussed in the next two sections.

4.1 Stress and displacement components in the core

The equilibrium equations for the core obtained in Sect. 4 as a result of implementing the principle of minimum total potential energy are as follows:

$$\begin{aligned}&(R_c + z_c)\frac{\partial\tau_{xz}^c(x,\theta,z_c)}{\partial z} + \tau_{xz}^c(x,\theta,z_c) = 0 \\ &(R_c + z_c)\frac{\partial\tau_{\theta z}^c(x,\theta,z_c)}{\partial z} + 2\tau_{\theta z}^c(x,\theta,z_c) = 0 \\ &(R_c + z_c)\frac{\partial\sigma_z^c(x,\theta,z_c)}{\partial z} + (R_c + z_c)\frac{\partial\tau_{xz}^c(x,\theta,z_c)}{\partial x} \\ &\quad + \frac{\partial\tau_{\theta z}^c(x,\theta,z_c)}{\partial\theta} + \sigma_z^c(x,\theta,z_c) = 0\end{aligned} \tag{12}$$

The expressions for the core stresses and displacements are determined by solving Eq. 12 along with Eqs. 3, 7 and using continuity of the transverse displacements (w) at the top and bottom interfaces, Eqs. 4c, 5c, and in-plane displacements (u, v) at the top interface, Eqs. 4a, b. The core stresses are obtained as follows:

$$\begin{aligned}&\tau_{xz}^c(x,\theta,z_c) = \frac{R_c}{R_c + z_c}T_{xz}^c(x,\theta); \\ &\tau_{\theta z}^c(x,\theta,z_c) = \frac{R_c^2}{(R_c + z_c)^2}T_{\theta z}^c(x,\theta); \\ &\sigma_z^c(x,\theta,z_c) = \frac{E_c}{(R_c + z_c)\ln\left(\frac{R_{tc}}{R_{bc}}\right)}\left(w_{0t}(x,\theta) - w_{0b}(x,\theta)\right) \\ &\qquad + \frac{R_c}{R_c + z_c}\left(R_c - z_c + \frac{h_c}{\ln\left(\frac{R_{tc}}{R_{bc}}\right)}\right)\frac{\partial T_{xz}^c(x,\theta)}{\partial x} \\ &\qquad + \frac{R_c^2}{R_c + z_c}\left(\frac{1}{R_c + z_c} + \frac{\frac{1}{R_{tc}} - \frac{1}{R_{bc}}}{\ln\left(\frac{R_{tc}}{R_{bc}}\right)}\right)\frac{\partial T_{\theta z}^c(x,\theta)}{\partial\theta}\end{aligned} \tag{13}$$

where $T_{\theta z}^c$ and T_{xz}^c which are called modified stresses at the mid-surface of the core are two new unknown parameters and must be obtained by solving the governing equations. Moreover, the displacements of the core are obtained in terms of the displacement field variables of the faces and the two new unknown parameters $T_{\theta z}^c$ and T_{xz}^c as follows:

$$u_c = u_{0t} + \frac{R_c}{G_c}\ln\left(\frac{R_c+z_c}{R_{tc}}\right)T^c_{xz} + \left(\frac{h_t}{2}+\frac{h_c}{2}-z_c\right)\frac{\partial w_{0t}}{\partial x} + \frac{R_c^2}{E_c}\left(\frac{h_c-2z_c}{2R_{tc}} + \ln\left(\frac{R_c+z_c}{R_{tc}}\right)\right)\frac{\partial^2 T^c_{\theta z}}{\partial x\partial\theta} + \frac{R_c}{Ec}\left(\frac{h_c^2}{8} - R_cR_{tc} - \frac{h_cz_c}{2} + \frac{z_c^2}{2} - R_c(R_c+z_c)\left(\ln\left(\frac{R_c+z_c}{R_{tc}}\right)-1\right)\right)\frac{\partial^2 T^c_{xz}}{\partial x^2} + \frac{z_c - h_c/2 - (R_c+z_c)\ln((R_c+z_c)/R_{tc})}{\ln(R_{tc}/R_{bc})} \times \left(\frac{\partial w_{0t}}{\partial x} - \frac{\partial w_{0b}}{\partial x} - \frac{h_cR_c^2}{R_{tc}R_{bc}E_c}\frac{\partial^2 T^c_{\theta z}}{\partial x\partial\theta} + \frac{R_c}{E_c}\left(R_c\ln\left(\frac{R_{bc}}{R_{tc}}\right)+h_c\right)\frac{\partial^2 T^c_{xz}}{\partial x^2}\right) \tag{14a}$$

$$v_c = \frac{R_c+z_c}{R_{tc}}\left(1-\frac{h_t}{2R_t}\right)v_{0t} + \frac{R_c^2}{2G_c}\left(\frac{R_c+z_c}{R_{tc}^2} - \frac{1}{R_c+z_c}\right)T^c_{\theta z} + \left(\frac{h_t-2R_t}{2R_tR_{tc}}(R_c+z_c)+1\right)\frac{\partial w_{0t}}{\partial\theta} + \frac{R_c^2}{E_c}\left(\frac{1}{R_{tc}} - \frac{1}{2(R_c+z_c)} - \frac{R_c+z_c}{2R_{tc}^2}\right)\frac{\partial^2 T^c_{\theta z}}{\partial\theta^2} + \frac{R_c}{E_c}\left(\frac{h_c}{2} - z_c + (R_c+z_c)\ln\left(\frac{R_c+z_c}{R_{tc}}\right)\right)\frac{\partial^2 T^c_{xz}}{\partial x\partial\theta} + \frac{1-(R_c+z_c)/R_{tc} + \ln((R_c+z_c)/R_{tc})}{\ln(R_{tc}/R_{bc})} \times \left(\frac{\partial w_{0t}}{\partial\theta} - \frac{\partial w_{0b}}{\partial\theta} - \frac{h_cR_c^2}{R_{tc}R_{bc}E_c}\frac{\partial^2 T^c_{\theta z}}{\partial\theta^2} + \frac{h_cR_c}{E_c}\frac{\partial^2 T^c_{xz}}{\partial x\partial\theta}\right) \tag{14b}$$

$$w_c = w_{0t} + \frac{R_c^2}{E_c}\frac{z_c - h_c/2}{R_{tc}(R_c+z_c)}\frac{\partial T^c_{\theta z}}{\partial\theta} + \frac{R_c}{E_c}\left(\frac{h_c}{2}-z_c\right)\frac{\partial T^c_{xz}}{\partial x} + \frac{\ln((R_c+z_c)/R_{tc})}{\ln(R_{tc}/R_{bc})}\left(w_{0t} - w_{0b} - \frac{h_cR_c^2}{R_{tc}R_{bc}E_c}\frac{\partial T^c_{\theta z}}{\partial\theta} + \frac{h_cR_c}{E_c}\frac{\partial T^c_{xz}}{\partial x}\right) \tag{14c}$$

4.2 Governing equations

Upon substitution of Eqs. 2, 6, 13, and 14a, b, c into the equilibrium equations of the faces obtained from implementing the principle of minimum total potential energy in Sect. 4, the governing coupled partial differential equations in terms of the displacement components are obtained as follows:

$$-\frac{C^t_{23}h_t}{R_t}\frac{\partial w_{0t}}{\partial\theta} - \frac{C^t_{33}h_t}{R_t}\frac{\partial^2 u_{0t}}{\partial\theta^2} - \frac{C^t_{23}h_t}{R_t}\frac{\partial^2 v_{0t}}{\partial\theta^2} - C^t_{12}h_t\frac{\partial w_{0t}}{\partial x} - 2C^t_{13}h_t\frac{\partial^2 u_{0t}}{\partial x\partial\theta} - h_t\left(C^t_{12}+C^t_{33}\right)\frac{\partial^2 v_{0t}}{\partial x\partial\theta} - C^t_{11}h_tR_t\frac{\partial^2 u_{0t}}{\partial x^2} - C^t_{13}h_tR_t\frac{\partial^2 v_{0t}}{\partial x^2} + R_cT^c_{xz} = 0 \tag{15}$$

$$-\frac{C^b_{23}h_b}{R_b}\frac{\partial w_{0b}}{\partial\theta} - \frac{C^b_{33}h_b}{R_b}\frac{\partial^2 u_{0b}}{\partial\theta^2} - \frac{C^b_{23}h_b}{R_b}\frac{\partial^2 v_{0b}}{\partial\theta^2} - C^b_{12}h_b\frac{\partial w_{0b}}{\partial x} - 2C^b_{13}h_b\frac{\partial^2 u_{0b}}{\partial x\partial\theta} - h_b\left(C^b_{12}+C^b_{33}\right)\frac{\partial^2 v_{0b}}{\partial x\partial\theta} - C^b_{11}h_bR_b\frac{\partial^2 u_{0b}}{\partial x^2} - C^b_{13}h_bR_b\frac{\partial^2 v_{0b}}{\partial x^2} - R_cT^c_{xz} = 0 \tag{16}$$

$$-\frac{C^t_{22}h_t}{R_t}\frac{\partial w_{0t}}{\partial\theta} - \frac{C^t_{23}h_t}{R_t}\frac{\partial^2 u_{0t}}{\partial\theta^2} - \frac{C^t_{22}h_t}{R_t}\left(\frac{h_t^2}{12R_t^2}+1\right)\frac{\partial^2 v_{0t}}{\partial\theta^2} + \frac{C^t_{22}h_t^3}{12R_t^3}\frac{\partial^3 w_{0t}}{\partial\theta^3} - C^t_{23}h_t\frac{\partial w_{0t}}{\partial x} - h_t\left(C^t_{12}+C^t_{33}\right)\frac{\partial^2 u_{0t}}{\partial x\partial\theta} - C^t_{23}h_t\left(2+\frac{h_t^2}{6R_t^2}\right)\frac{\partial^2 v_{0t}}{\partial x\partial\theta} + \frac{C^t_{23}h_t^3}{4R_t^2}\frac{\partial^3 w_{0t}}{\partial x\partial\theta^2} - C^t_{13}h_tR_t\frac{\partial^2 u_{0t}}{\partial x^2} - C^t_{33}h_t\left(\frac{h_t^2}{12R_t}+R_t\right)\frac{\partial^2 v_{0t}}{\partial x^2} + \frac{h_t^3}{12R_t}\left(C^t_{12}+2C^t_{33}\right)\frac{\partial^3 w_{0t}}{\partial x^2\partial\theta} + \frac{C^t_{13}h_t^3}{12}\frac{\partial^3 w_{0t}}{\partial x^3} + \frac{R_c^2}{R_t}T^c_{\theta z} = 0 \tag{17}$$

$$-\frac{C^b_{22}h_b}{R_b}\frac{\partial w_{0b}}{\partial\theta} - \frac{C^b_{23}h_b}{R_b}\frac{\partial^2 u_{0b}}{\partial\theta^2} - \frac{C^b_{22}h_b}{R_b}\left(\frac{h_b^2}{12R_b^2}+1\right)\frac{\partial^2 v_{0b}}{\partial\theta^2} + \frac{C^b_{22}h_b^3}{12R_b^3}\frac{\partial^3 w_{0b}}{\partial\theta^3} - C^b_{23}h_b\frac{\partial w_{0b}}{\partial x} - h_b\left(C^b_{12}+C^b_{33}\right)\frac{\partial^2 u_{0b}}{\partial x\partial\theta} - C^b_{23}h_b\left(2+\frac{h_b^2}{6R_b^2}\right)\frac{\partial^2 v_{0b}}{\partial x\partial\theta} + \frac{C^b_{23}h_b^3}{4R_b^2}\frac{\partial^3 w_{0b}}{\partial x\partial\theta^2} - C^b_{13}h_bR_b\frac{\partial^2 u_{0b}}{\partial x^2} - C^b_{33}h_b\left(\frac{h_b^2}{12R_b}+R_b\right)\frac{\partial^2 v_{0b}}{\partial x^2} + \frac{h_b^3}{12R_b}\left(C^b_{12}+2C^b_{33}\right)\frac{\partial^3 w_{0b}}{\partial x^2\partial\theta} + \frac{C^b_{13}h_b^3}{12}\frac{\partial^3 w_{0b}}{\partial x^3} - \frac{R_c^2}{R_b}T^c_{\theta z} = 0 \tag{18}$$

$$R_tq_t + \left(\frac{E_c}{\ln(R_{tc}/R_{bc})} + \frac{C^t_{22}h_t}{R_t}\right)w_{0t} - \frac{E_c}{\ln(R_{tc}/R_{bc})}w_{0b} + \frac{C^t_{23}h_t}{R_t}\frac{\partial u_{0t}}{\partial\theta} + \frac{C^t_{22}h_t}{R_t}\frac{\partial v_{0t}}{\partial\theta} - \frac{C^t_{22}h_t^3}{12R_t^3}\frac{\partial^3 v_{0t}}{\partial\theta^3} + \frac{C^t_{22}h_t^3}{12R_t^3}\frac{\partial^4 w_{0t}}{\partial\theta^4} + C^t_{12}h_t\frac{\partial u_{0t}}{\partial x} + C^t_{23}h_t\frac{\partial v_{0t}}{\partial x} - \frac{C^t_{23}h_t^3}{4R_t^2}\frac{\partial^3 v_{0t}}{\partial x\partial\theta^2} + \frac{C^t_{23}h_t^3}{3R_t^2}\frac{\partial^4 w_{0t}}{\partial x\partial\theta^3} - \frac{h_t^3}{12R_t}\left(2C^t_{33}+C^t_{12}\right)\frac{\partial^3 v_{0t}}{\partial x^2\partial\theta} + \frac{h_t^3}{6R_t}\left(2C^t_{33}+C^t_{12}\right)\frac{\partial^4 w_{0t}}{\partial x^2\partial\theta^2} - \frac{C^t_{13}h_t^3}{12}\frac{\partial^3 v_{0t}}{\partial x^3} + \frac{C^t_{13}h_t^3}{3}\frac{\partial^4 w_{0t}}{\partial x^3\partial\theta} + \frac{C^t_{11}h_t^3R_t}{12}\frac{\partial^4 w_{0t}}{\partial x^4} + \frac{R_c^2}{R_{tc}}\left(1-\frac{h_t}{2R_t}-\frac{h_c}{R_{bc}\ln(R_{tc}/R_{bc})}\right)\frac{\partial \mathrm{T}^c_{\theta z}}{\partial\theta} + R_c\left(\frac{h_c}{\ln(R_{tc}/R_{bc})} - \frac{h_t}{2} - R_{tc}\right)\frac{\partial \mathrm{T}^c_{xz}}{\partial x} = 0 \tag{19}$$

$$
\begin{aligned}
&R_b q_b - \frac{E_c}{\ln(R_{tc}/R_{bc})} w_{0t} + \left(\frac{E_c}{\ln(R_{tc}/R_{bc})} + \frac{C_{22}^b h_b}{R_b}\right) w_{0b} \\
&+ \frac{C_{23}^b h_b}{R_b}\frac{\partial u_{0b}}{\partial\theta} + \frac{C_{22}^b h_b}{R_b}\frac{\partial v_{0b}}{\partial\theta} \\
&- \frac{C_{22}^b h_b^3}{12R_b^3}\frac{\partial^3 v_{0b}}{\partial\theta^3} + \frac{C_{22}^b h_b^3}{12R_b^3}\frac{\partial^4 w_{0b}}{\partial\theta^4} + C_{12}^b h_b \frac{\partial u_{0b}}{\partial x} + C_{23}^b h_b \frac{\partial v_{0b}}{\partial x} \\
&- \frac{C_{23}^b h_b^3}{4R_b^2}\frac{\partial^3 v_{0b}}{\partial x\partial\theta^2} + \frac{C_{23}^b h_b^3}{3R_b^2}\frac{\partial^4 w_{0b}}{\partial x\partial\theta^3} \\
&- \frac{h_b^3}{12R_b}(2C_{33}^b + C_{12}^b)\frac{\partial^3 v_{0b}}{\partial x^2\partial\theta} + \frac{h_b^3}{6R_b}(2C_{33}^b + C_{12}^b)\frac{\partial^4 w_{0b}}{\partial x^2\partial\theta^2} \\
&- \frac{C_{13}^b h_b^3}{12}\frac{\partial^3 v_{0b}}{\partial x^3} + \frac{C_{13}^b h_b^3}{3}\frac{\partial^4 w_{0b}}{\partial x^3\partial\theta} \\
&+ \frac{C_{11}^b h_b^3 R_b}{12}\frac{\partial^4 w_{0b}}{\partial x^4} - \frac{R_c^2}{R_{bc}}\left(1 + \frac{h_b}{2R_b} - \frac{h_c}{R_{bc}\ln(R_{tc}/R_{bc})}\right)\frac{\partial T_{\theta z}^c}{\partial\theta} \\
&- R_c\left(\frac{h_c}{\ln(R_{tc}/R_{bc})} + \frac{h_b}{2} - R_{bc}\right)\frac{\partial T_{xz}^c}{\partial x} = 0
\end{aligned}
\tag{20}
$$

Also the corresponding boundary conditions are presented in Appendix A and B for straight edges ($\theta = 0,\ \beta$) and curved edges ($x = 0,\ L$), respectively.

To obtain a complete and consistent set of governing equations, two other equations are needed. These equations are the continuity of the in-plane displacements (u, v) at the bottom interface, Eqs. 5a, b, which are not implemented yet and using the expressions for u_c and v_c, Eqs. 14a, b, are obtained as follows:

$$
\begin{aligned}
&u_{0t} - u_{0b} + \frac{R_c}{G_c}\ln\left(\frac{R_{bc}}{R_{tc}}\right)T_{xz}^c + \frac{h_b}{2}\frac{\partial w_{0b}}{\partial x} + \left(h_c + \frac{h_t}{2}\right)\frac{\partial w_{0t}}{\partial x} \\
&+ \frac{R_c^2}{E_c}\ln\left(\frac{R_{bc}}{R_{tc}}\right)\frac{\partial^2 T_{\theta z}^c}{\partial x\partial\theta} + \frac{R_c}{Ec}\left(\frac{h_c^2}{2} - R_c h_c - R_c R_{bc}\ln\left(\frac{R_{bc}}{R_{tc}}\right)\right) \\
&\times\frac{\partial^2 T_{xz}^c}{\partial x^2} + \left(R_{bc} - \frac{h_c}{\ln(R_{tc}/R_{bc})}\right)\left(\frac{\partial w_{0t}}{\partial x} - \frac{\partial w_{0b}}{\partial x} - \frac{h_c R_c^2}{R_{tc}R_{bc}E_c}\frac{\partial^2 T_{\theta z}^c}{\partial x\partial\theta}\right) \\
&+ \frac{R_c}{Ec}\left(R_c\ln\left(\frac{R_{bc}}{R_{tc}}\right) + \right)\frac{\partial^2 T_{xz}^c}{\partial x^2} = 0
\end{aligned}
\tag{21}
$$

$$
\begin{aligned}
&\frac{R_{bc}}{R_{tc}}\left(1 - \frac{h_t}{2R_t}\right)v_{0t} - \left(1 + \frac{h_b}{2R_b}\right)v_{0b} + \frac{R_c^2}{2G_c}\left(\frac{R_{bc}}{R_{tc}^2} - \frac{1}{R_{bc}}\right)T_{\theta z}^c \\
&+ \left(\frac{h_t R_{bc}}{2R_t R_{tc}} - \frac{R_{bc}}{R_{tc}} + 1\right)\frac{\partial w_{0t}}{\partial\theta} + \frac{h_b}{2R_b}\frac{\partial w_{0b}}{\partial\theta} \\
&+ \frac{R_c^2}{E_c}\left(\frac{1}{R_{tc}} - \frac{1}{2R_{bc}} - \frac{R_{bc}}{2R_{tc}^2}\right)\frac{\partial^2 T_{\theta z}^c}{\partial\theta^2} \\
&+ \frac{R_c}{E_c}\left(h_c + R_{bc}\ln\left(\frac{R_{bc}}{R_{tc}}\right)\right)\frac{\partial^2 T_{xz}^c}{\partial x\partial\theta} \\
&+ \frac{1 - R_{bc}/R_{tc} + \ln(R_{bc}/R_{tc})}{\ln(R_{tc}/R_{bc})} \\
&\left(\frac{\partial w_{0t}}{\partial\theta} - \frac{\partial w_{0b}}{\partial\theta} - \frac{h_c R_c^2}{R_{tc}R_{bc}E_c}\frac{\partial^2 T_{\theta z}^c}{\partial\theta^2} + \frac{h_c R_c}{E_c}\frac{\partial^2 T_{xz}^c}{\partial x\partial\theta}\right) = 0
\end{aligned}
\tag{22}
$$

It is seen that the governing equations in (15) through (22) are in terms of eight unknowns; i.e., u_{0t}, u_{0b}, v_{0t}, v_{0b}, w_{0t}, w_{0b}, T_{xz}^c, and $T_{\theta z}^c$. The solution procedure for these equations along with the associated boundary conditions in 29, 30, 31, 32, 33, 34, 35, 36 and 45, 46, 47, 48, 49, 50, 51, 52 is presented in the next section.

4.3 Solution procedure

For solving the obtained equations, the HDQM is used. In this method, the partial derivative of a function, with respect to a spatial variable at a given discrete point, is approximated by a linear summation of weighted function values at all discrete points chosen in the solution domain of the spatial variable. The domain of the considered shell ($0 < x < L,\ 0 < \theta < \beta$) is discretized by $N_x \times N_\theta$ grid points along x and θ coordinates. If $F(x,\ \theta)$ represents either of the functions u_{0t}, u_{0b}, v_{0t}, v_{0b}, w_{0t}, w_{0b}, T_{xz}^c, and $T_{\theta z}^c$ within the shell domain, then the partial derivatives of $F(x,\ \theta)$ with respect to x and θ at the point $(x_i,\ \theta_j)$ can be expressed discretely as [17]:

$$
\frac{d^n F(x_i,\theta_j)}{\mathrm{d}x^n} = \sum_{k=1}^{N_x} A_{ik}^{(n)} F(x_k,\theta_j); \quad n = 1,2,\ldots,N_x - 1;
\tag{23}
$$

$$
\frac{d^m F(x_i,\theta_j)}{\mathrm{d}\theta^m} = \sum_{l=1}^{N_\theta} B_{jl}^{(m)} F(x_i,\theta_l); \quad m = 1,2,\ldots,N_\theta - 1;
\tag{24}
$$

$$
\frac{d^{n+m} F(x_i,\theta_j)}{\mathrm{d}x^n \mathrm{d}\theta^m} = \sum_{k=1}^{N_x}\sum_{l=1}^{N_\theta} A_{ik}^{(n)} B_{jl}^{(m)} F(x_k,\theta_l) \quad \begin{array}{l} ; \quad n = 1,2,\ldots,N_x - 1; \\ ; \quad m = 1,2,\ldots,N_\theta - 1; \end{array}
\tag{25}
$$

where $A_{ik}^{(n)}$ and $B_{jl}^{(m)}$ are the weighting coefficients in conjunction with the order of partial derivative of $F(x,\ \theta)$ with respect to x, i.e., n and the order of derivative with respect to θ, i.e., m at the discrete point $(x_i,\ \theta_j)$, respectively. Here, the grid points are selected based on the Chebyshev polynomials. The description of HDQ method and how to choose the positions of the grid points using Chebyshev polynomials can be found in detail in [17]. Now, Eqs. 23 through 25 are utilized to discretize the coupled governing equations in 15, 16, 17, 18, 19, 20, 21, 22 along with the corresponding boundary conditions in 29, 30, 31, 32, 33, 34, 35, 36 and 45, 46, 47, 48, 49, 50, 51, 52. However, for the sake of brevity, only the discretized form of Eq. 15 at the discrete point $(x_i,\ \theta_j)$ is presented here, as follows:

Table 1 Transverse displacement of the shell at $x = L/2$ and $\theta = \beta/2$, for lateral pressure of $q_t = 100$ Pa

B.C.s	w_t at $z_t = 0$			w_c at $z_c = 0$			w_b at $z_b = 0$		
	FEM (10^{-7} m)	HOT-HDQM (10^{-7} m)	%disc.[a]	FEM (10^{-7} m)	HOT-HDQM (10^{-7} m)	%disc.	FEM (10^{-7} m)	HOT-HDQM (10^{-7} m)	%disc.
CCCC	–4.3856	–4.4025	*–0.385*	–4.3720	–4.3719	*0.003*	–4.3572	–4.2785	*1.806*
CCSS	–9.6915	–9.9524	*–2.692*	–9.6850	–9.9111	*–2.334*	–9.6736	–9.8640	*–1.969*
SSCS	–15.891	–16.387	*–3.122*	–15.894	–16.327	*–2.725*	–15.887	–16.258	*–2.335*
SSSS	–18.525	–18.915	*–2.105*	–18.527	–18.853	*–1.759*	–18.520	–18.781	*–1.412*

[a] %disc. = [(FEM)−(HOT-HDQM)]/(FEM) × 100

$$
\begin{aligned}
&-\frac{C^t_{23}h_t}{R_t}\sum_{l=1}^{N_\theta}B^{(1)}_{jl}w_{0t_{i,l}}-\frac{C^t_{33}h_t}{R_t}\sum_{l=1}^{N_\theta}B^{(2)}_{jl}u_{0t_{i,l}}\\
&-\frac{C^t_{23}h_t}{R_t}\sum_{l=1}^{N_\theta}B^{(2)}_{jl}v_{0t_{i,l}}-C^t_{12}h_t\sum_{k=1}^{N_x}A^{(1)}_{ik}w_{0t_{k,j}}\\
&-2C^t_{13}h_t\sum_{k=1}^{N_x}\sum_{l=1}^{N_\theta}A^{(1)}_{ik}B^{(1)}_{jl}u_{0t_{k,l}}\\
&-h_t\left(C^t_{12}+C^t_{33}\right)\sum_{k=1}^{N_x}\sum_{l=1}^{N_\theta}A^{(1)}_{ik}B^{(1)}_{jl}v_{0t_{k,l}}\\
&-C^t_{11}h_tR_t\sum_{k=1}^{N_x}A^{(2)}_{ik}u_{0t_{k,l}}-C^t_{13}h_tR_t\sum_{k=1}^{N_x}A^{(2)}_{ik}v_{0t_{k,l}}+R_cT^c_{xz_{i,j}}=0
\end{aligned}
\tag{26}
$$

For any sort of boundary conditions (clamped, simply supported or free, see Appendix A and B), after separating the domain and the boundary degrees of freedom (DOF), the following assembled matrix equations are obtained:

$$
\begin{bmatrix}[K_{bb}] & [K_{bd}]\\ [K_{db}] & [K_{dd}]\end{bmatrix}\begin{Bmatrix}\{d^b\}\\ \{d^d\}\end{Bmatrix}=\begin{Bmatrix}0\\ \{P\}\end{Bmatrix}
\tag{27}
$$

where $\{d^b\}$ and $\{d^d\}$ represent the boundary and domain DOF, respectively, and $\{P\}$ is the load vector. After doing some mathematical simplifications on Eq. 27, the displacement components can be calculated by solving the following relation:

$$
\left[[K_{dd}]-[K_{db}][K_{bb}]^{-1}[K_{bd}]\right]\{d^d\}=\{P\}
\tag{28}
$$

Based on the above-outlined formulations, and using the MALAB program solver, a self-developed computer program is written by which the displacements, strains and stresses in different points of the shell faces and core can be obtained. Again it should be emphasized that no limitations on the type of boundary conditions and loading exist when solving these equations.

5 Results and discussions

Primarily, to investigate the convergence of HOT-HDQ method, several cases with different number of grid points were examined which for brevity are not presented here. The outcome of this convergence study is that selecting a grid with minimum 21 × 21 points will yield a stable answer in any problem under consideration. Therefore, in all up-coming case studies, this gird scheme has been used. The results obtained based on the HOT-HDQM are compared with those obtained from an FEM model in ANSYS software comprising 11892 of 3-D 20-noded brick type elements with total number of nodes of 85,273.

5.1 Case study 1: evaluation of proper functionality and verification

A cylindrical sandwich shell with different boundary conditions subjected to a uniform lateral pressure is considered. The geometrical parameters are $L = 0.9$ m, $R = 1.2$ m, $\beta = 35°$, $h_t = 1$ mm, $h_b = 1$ mm, $h_c = 10$ - mm (see Fig. 1). Also, the structural steel with $E_f = 210$ GPa and $v_f = 0.3$ has been chosen for both face materials. The core material is AirexR63.50 [27] with $E_c = 37.5$ MPa and $G_c = 14.05$ MPa. The results for central transverse displacement w of the shell under a uniform lateral pressure of $q_t = 100$ Pa are compared with those obtained using FEM analysis in Table 1. In this table, four combinations of simply supported (S) and clamped (C) boundary conditions for four edges are considered (for example, CCSS denotes a cylindrical shell with one clamped curved edge, one clamped axial edge, one simply supported curved edge, and one simply supported axial edge).

The comparison of the results in Table 1 shows a very good agreement between the HOT-HDQM and FEM results.

The variations of the transverse displacement w in the core mid-surface along θ and x directions are presented in Fig. 2, for the shell with all edges clamped and under a uniform pressure of $q_t = 1$ kPa. For this shell, distributions of normal stress σ_z and transverse shear stresses τ_{xz} and $\tau_{\theta z}$ of the core mid-surface along x and θ directions are shown in Figs. 3, 4, respectively. In addition, in-plane normal stress σ_θ of the top surface of the shell along θ direction and in-plane normal stress σ_x of the bottom surface of the

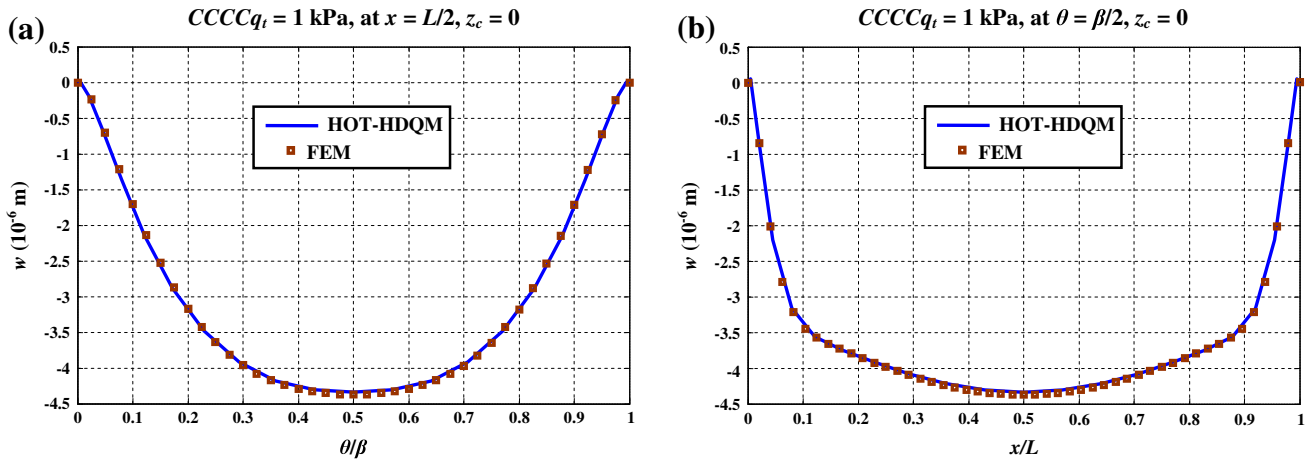

Fig. 2 Transverse displacement in the core mid-surface for uniform loading along **a** θ and **b** x directions

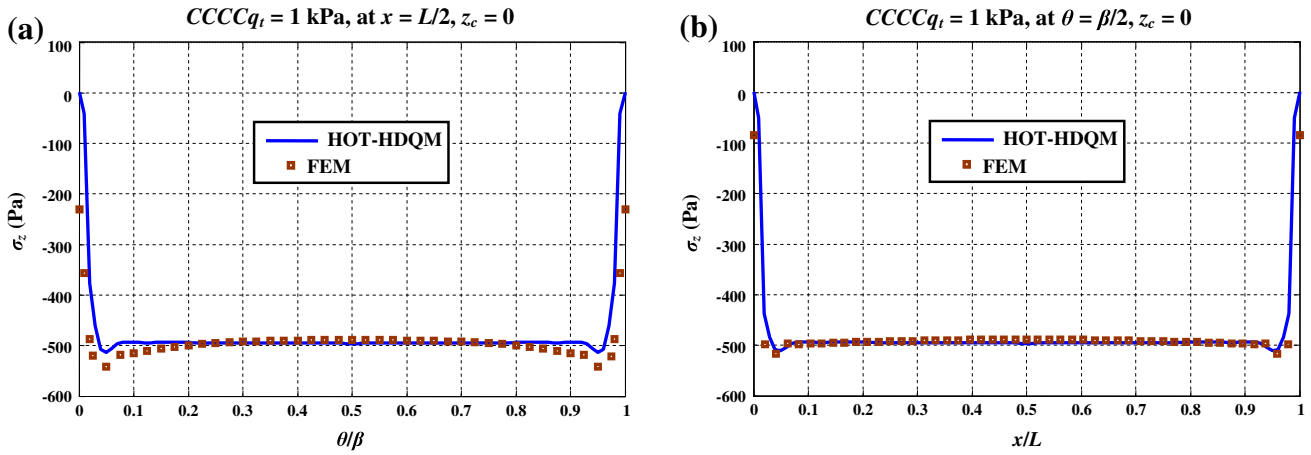

Fig. 3 Transverse normal stress σ_z in the core mid-surface for uniform loading along **a** θ and **b** x directions

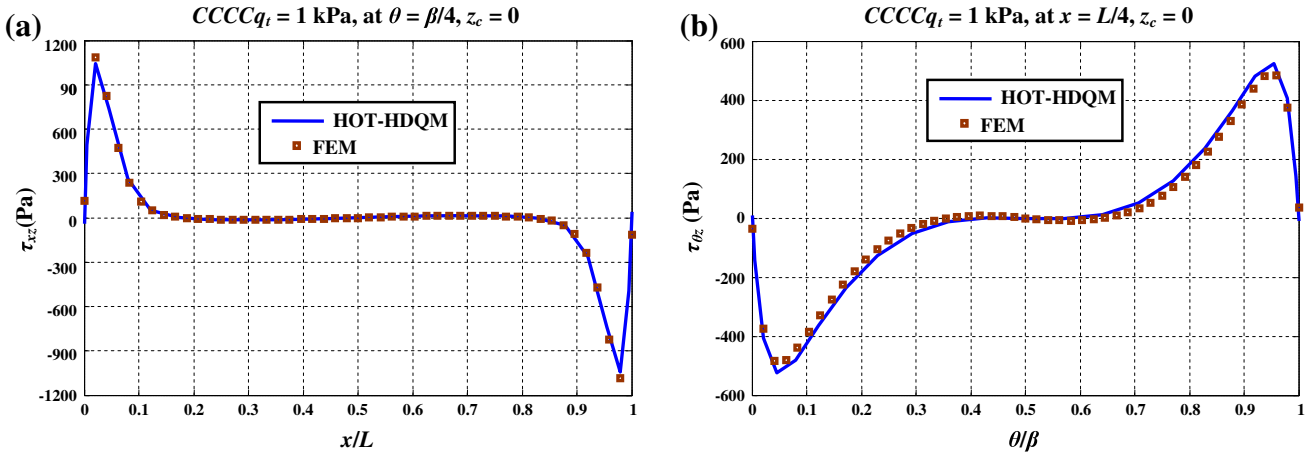

Fig. 4 Transverse shear stresses **a** τ_{xz} along x direction and **b** $\tau_{\theta z}$ along θ direction in the core mid-surface for uniform loading

shell along x direction are shown in Fig. 5. In all above cases, the FEM results are also shown along with the HOT-HDQM results. A close inspection of these results indicates a very good agreement between the HOT-HDQM and FEM results. Note that based on the Saint-Venant's principle, the results near to the boundaries cannot be trusted.

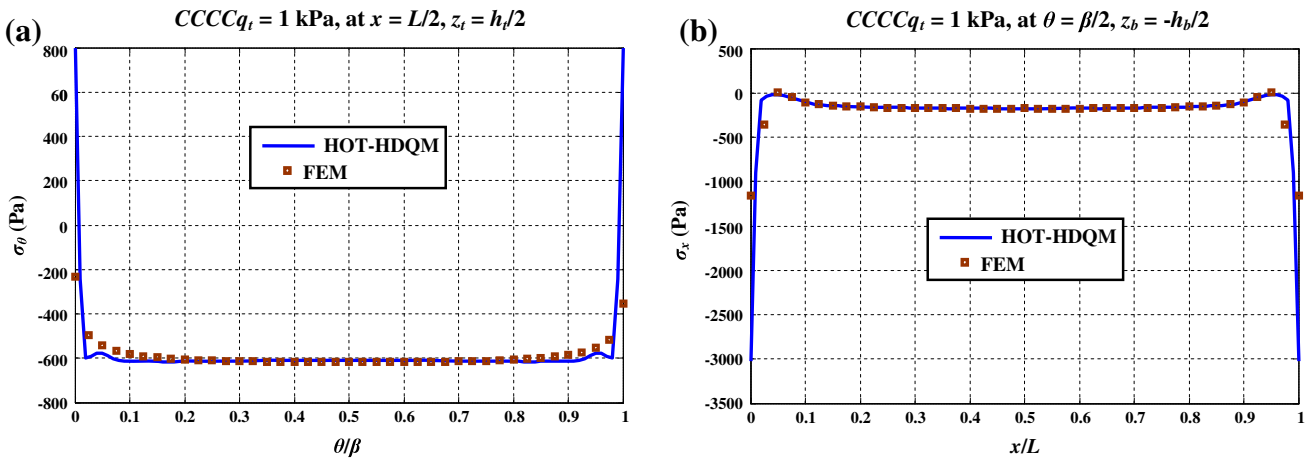

Fig. 5 **a** In-plane normal stress σ_θ of *top* surface of the shell along θ direction and **b** in-plane normal stress σ_x of *bottom* surface of the shell along x direction for uniform loading

Table 2 Transverse displacement, w (10^{-6} m) at $x = L/3$, $\theta = \beta/3$ and $z_c = 0$

E_f/E_c	$h_c/h_f = 5$			$h_c/h_f = 10$			$h_c/h_f = 20$		
	HOT-HDQM	FEM	%disc.	HOT-HDQM	FEM	%disc.	HOT-HDQM	FEM	%disc.
525	–3.7699	–3.8474	–2.01	–3.7711	–3.9118	–3.60	–3.6201	–3.7679	–3.92
1,050	–3.6753	–3.7011	–0.70	–3.7385	–3.7921	–1.41	–3.7295	–3.7828	–1.41
2,625	–3.5024	–3.4856	0.48	–3.6033	–3.5991	0.12	–3.6973	–3.6917	0.15
5,250	–3.3586	–3.3225	1.09	–3.4707	–3.4460	0.72	–3.5955	–3.5706	0.70
10,500	–3.2151	–3.1682	1.48	–3.3282	–3.2908	1.14	–3.4661	–3.4290	1.08

It should be further clarified that for the case of cylindrical sandwich shell with *CCCC* type of boundary conditions under a uniform pressure, the CPU time used by the self-developed program based on the implementation of HOT-HDQM reveals a minimum 50.6 % saving in CPU time with respect to the FEM model. Furthermore, it has been verified that upon equal number of nodes in a specified grid size, the developed program based on HOT-HDQ method leads to a more accurate result than FEM. Note that this advantage of the DQ methods over FEM has been frequently reported by other researchers as well [17, 21].

5.2 Case study 2: effects of core flexibility

To investigate the effect of core flexibility, a cylindrical sandwich shell with clamped edges (CCCC) under a uniform pressure of $q_t = 1$ kPa is considered. Furthermore, the geometry of the shell comprises the following parameters; $L = 0.9$ m, $R = 1.2$ m, $\beta = 60°$, $h_t = 1$ mm, $h_b = 1$ mm, and h_c has three different values $h_c = 5$ mm, $h_c = 10$ mm, and $h_c = 20$ mm. The faces are made of structural steel with the same mechanical properties as the one considered in Sect. 5.1. Nonetheless, several isotropic materials are selected for the core material with the values of their E_c, varying in the range of 20–400 MPa (for foams like PVC and PU: $E_c < 400$ MPa). The variation of transverse displacement w and transverse normal stress σ_z at the core mid-surface, in-plane normal stress σ_x on the external surface of the shell and in-plane normal stress σ_θ on the internal surface of the shell are listed in Table 2, 3, 4, and 5, respectively, for five different ratios of E_f/E_c and three different ratios of h_c/h_f.

As indicated in Tables 2, 3, 4, 5, comparison of these results shows a very good agreement between HOT-HDQM and FEM model (The greatest error is 6.91 % for σ_x). These results show that by increasing the ratios of h_c/h_f, the accuracy of HOT-HDQM decreases. It may be due to ignoring the in-plane stresses in the core modeling based on the HOT. Moreover, no specific trend in the errors of the shell displacement and stresses can be seen when E_f/E_c ratios are changed.

5.3 Case study 3: effects of geometric parameters

Here, two important ratios: the core to the face thickness ratio (h_c/h_f) and the ratio of shell curvature to thickness (R/h) are

Table 3 Transverse normal stress, σ_z (Pa) at $x = L/3$, $\theta = \beta/3$ and $z_c = 0$

E_f/E_c	$h_c/h_f = 5$			$h_c/h_f = 10$			$h_c/h_f = 20$		
	HOT-HDQM	FEM	%disc.	HOT-HDQM	FEM	%disc.	HOT-HDQM	FEM	%disc.
525	–500.55	–490.51	2.05	–499.29	–478.88	4.26	–499.04	–467.32	6.79
1,050	–500.43	–494.23	1.25	–500.18	–487.85	2.53	–500.78	–482.67	3.75
2,625	–499.64	–498.57	0.21	–499.23	–496.59	0.53	–498.63	–496.13	0.50
5,250	–497.86	–500.05	–0.44	–495.67	–499.06	–0.68	–491.26	–498.8	–1.51
10,500	–493.94	–499.29	–1.07	–487.70	–497.36	–1.94	–475.31	–494.38	–3.86

Table 4 In-plane normal stress, σ_x (Pa) at $x = L/3$, $\theta = \beta/3$ and $z_t = h_t/2$

E_f/E_c	$h_c/h_f = 5$			$h_c/h_f = 10$			$h_c/h_f = 20$		
	HOT-HDQM	FEM	%disc.	HOT-HDQM	FEM	%disc.	HOT-HDQM	FEM	%disc.
525	–179,770	–186,320	–3.52	–190,190	–201,500	–5.61	–198,150	–212,850	–6.91
1,050	–179,630	–183,470	–2.09	–185,090	–190,920	–3.05	–188,980	–196,010	–3.59
2,625	–177,500	–178,460	–0.54	–179,720	–181,120	–0.77	–181,270	–182,620	–0.74
5,250	–175,530	–174,930	0.34	–177,950	–177,030	0.52	–180,840	–178,910	1.08
10,500	–174,180	–172,380	1.04	–178,160	–174,960	1.83	–184,630	–178,640	3.35

Table 5 In-plane normal stress, σ_θ (Pa) at $x = L/3$, $\theta = \beta/3$ and $z_b = -h_b/2$

E_f/E_c	$h_c/h_f = 5$			$h_c/h_f = 10$			$h_c/h_f = 20$		
	HOT-HDQM	FEM	%disc.	HOT-HDQM	FEM	%disc.	HOT-HDQM	FEM	%disc.
525	–592,840	–589,700	0.53	–579,700	–565,510	2.51	–545,420	–519,390	5.01
1,050	–597,340	–593,780	0.60	–591,330	–579,960	1.96	–575,210	–558,580	2.98
2,625	–599,830	–599,870	–0.01	–596,430	–593,820	0.44	–589,640	–589,980	–0.06
5,250	–599,940	–602,960	–0.50	–595,130	–598,960	–0.64	–586,290	–598,650	–2.06
10,500	–597,050	–603,290	–1.03	–587,930	–598,760	–1.81	–570,590	–596,530	–4.35

Table 6 Transverse and in-plane normal stresses at $x = L/3$ and $\theta = \beta/4$

h_c/h_f	σ_z(Pa) at $z_c = 0$			σ_x (Pa) at $z_b = -h_b/2$			σ_θ (Pa) at $z_t = h_t/2$		
	HOT-HDQM	FEM	%disc.	HOT-HDQM	FEM	%disc.	HOT-HDQM	FEM	%disc.
5	–497.58	–494.39	0.64	–165,620	–169,770	–2.44	–605,090	610,370	–0.87
10	–495.42	–494.17	0.25	–162,830	–166,600	–2.26	–610,410	–611,210	–0.13
20	–491.03	–495.40	–0.88	–157,480	–161,520	–2.50	–619,010	–615,790	0.52
40	–482.30	–499.12	–3.37	–149,970	–154,110	–2.69	–631,680	–601,980	4.93

studied. To study the core to the face thickness ratio, a cylindrical sandwich shell with clamped edges (CCCC) subjected to a uniform lateral pressure of $q_t = 1$ kPa is considered. The geometrical parameters are $L = 0.9$ m, $R = 1.2$ m, $\beta = 60°$, $h_t = 1$ mm, $h_b = 1$ mm and h_c has four different values 5, 10, 20, and 40 mm. Also, the faces and the core are made of the structural steel and AirexR63.50, respectively, whose properties are given in Sect. 5.1.

The results for transverse normal stress σ_z of the core mid-surface, in-plane normal stress σ_x of the top surface of

Table 7 Transverse and in-plane normal stresses at $x = L/3$ and $\theta = \beta/3$

R/h	σ_z(Pa) at $z_c = 0$			σ_x (Pa) at $z_b = -h_b/2$			σ_θ (Pa) at $z_t = h_t/2$		
	HOT-HDQM	FEM	%disc.	HOT-HDQM	FEM	%disc.	HOT-HDQM	FEM	%disc.
500	–491.31	–492.44	–0.23	–382,050	–394,710	–3.21	–2,622,200	–2,655,800	–1.27
100	–494.60	–498.81	–0.84	–154,110	–155,000	–0.57	–560,640	–555,130	0.99
50	–468.37	–490.62	–4.54	–76,247	–80,463	–5.24	–298,760	–285,660	4.59
20	–340.23	–435.95	–22.0	–20,898	–27,781	–24.8	–153,300	–131,610	16.5

the shell, and in-plane normal stress σ_θ of the bottom surface of the shell for four different thickness ratios at specified positions are presented in Table 6. A very good agreement between HOT-HDQM and FEM is observed. Furthermore, it is seen that by increasing the ratios of h_c/h_f, the accuracy of HOT-HDQM decreases which was also reported in the second case study.

To study the effect of the curvature to thickness ratio, a cylindrical sandwich shell with clamped edges (CCCC) subjected to a uniform lateral pressure of $q_t = 1$ kPa is considered. The geometrical parameters are $L = 0.9$ m, $\beta = 60°$, $h_t = 1$ mm, $h_b = 1$ mm, $h_c = 10$ mm and the problem has been solved for four different values of R/h 20, 50, 100, and 500. Also, the faces and the core are made of structural steel and AirexR63.50, respectively, with the same mechanical properties as those used in the case study 1.

The results for transverse normal stress σ_z on the core mid-surface, in-plane normal stress σ_x on the external surface of shell, and in-plane normal stress σ_θ on the internal surface of shell are given in Table 7. This table shows that by decreasing the curvature to thickness ratio, the difference between HOT-HDQM and FEM increases. This, on the other hand, is due to the assumptions of Love–Kirchhoff shell theory (used here in modeling of the faces) which are valid for thin shallow shells.

6 Conclusion

Cylindrical sandwich shells under general type of distributive lateral loadings are modeled based on a HOT of sandwich structures. The faces are modeled as thin cylindrical shells obeying the Kirchhoff–Love assumptions. For the core material, it is assumed to be thick and the in-plane stresses are negligible. The governing equations are derived using the principle of minimum total potential energy and solved using HDQM. The obtained results using HOT-HDQM are compared with the results out of the finite element method. Based on this study, the followings are concluded:

- In using HOT-HDQM for static analysis of sandwich shells, there are no limits on type of boundary conditions and loadings.
- The convergence of the HOT-HDQM is faster than FEM and the calculation cost for the HOT-HDQM is less than FEM.
- HOT-HDQM neglects the in-plane strains and stresses in the core and, therefore, it is expected that less accurate results be obtained in comparison with FEM. However, the results show that for low stiffness cores, this assumption is a valid assumption and has no significant effect in the results.
- For sandwich panels having low stiffness cores with small ratios of the core to the face thickness, there is a good agreement between HOT-HDQM and finite element results.
- Comparison of the results obtained based on HOT-HDQM and FEM shows that by increasing the core to the face thickness ratio and the curvature to thickness ratio, the accuracy of HOT-HDQM decreases.

Appendix A

Boundary conditions, on $\theta = 0$, β.

$$\delta u_{0t} A U_{0t} = 0 \tag{29}$$

$$\delta u_{0b} A U_{0b} = 0 \tag{30}$$

$$\delta v_{0t} A V_{0t} = 0 \tag{31}$$

$$\delta v_{0b} A V_{0b} = 0 \tag{32}$$

$$\delta w_{0t} A W_{0t} = 0 \tag{33}$$

$$\delta w_{0b} A W_{0b} = 0 \tag{34}$$

$$\delta \frac{\partial w_{0t}}{\partial \theta} A D W_{0t} = 0 \tag{35}$$

$$\delta \frac{\partial w_{0b}}{\partial \theta} A D W_{0b} = 0 \tag{36}$$

where.

$$AU_{0t} = \frac{C_{23}^t h_t}{R_t} w_{0t} + \frac{C_{33}^t h_t}{R_t}\frac{\partial u_{0t}}{\partial \theta} + \frac{C_{23}^t h_t}{R_t}\frac{\partial v_{0t}}{\partial \theta} + C_{13}^t h_t \frac{\partial u_{0t}}{\partial x} + C_{33}^t h_t \frac{\partial v_{0t}}{\partial x} \quad (37)$$

$$AU_{0b} = \frac{C_{23}^b h_b}{R_b} w_{0b} + \frac{C_{33}^b h_b}{R_b}\frac{\partial u_{0b}}{\partial \theta} + \frac{C_{23}^b h_b}{R_b}\frac{\partial v_{0b}}{\partial \theta} + C_{13}^b h_b \frac{\partial u_{0b}}{\partial x} + C_{33}^b h_b \frac{\partial v_{0b}}{\partial x} \quad (38)$$

$$AV_{0t} = \frac{C_{22}^t h_t}{R_t} w_{0t} + \frac{C_{23}^t h_t}{R_t}\frac{\partial u_{0t}}{\partial \theta} + \frac{C_{22}^t h_t}{R_t}\left(1 + \frac{h_t^2}{12R_t^2}\right)\frac{\partial v_{0t}}{\partial \theta} - \frac{C_{22}^t h_t^3}{12R_t^3}\frac{\partial^2 w_{0t}}{\partial \theta^2} + C_{12}^t h_t \frac{\partial u_{0t}}{\partial x} + C_{23}^t h_t \left(1 + \frac{h_t^2}{12R_t^2}\right)\frac{\partial v_{0t}}{\partial x} - \frac{C_{23}^t h_t^3}{6R_t^2}\frac{\partial^2 w_{0t}}{\partial x \partial \theta} - \frac{C_{12}^t h_t^3}{12R_t}\frac{\partial^2 w_{0t}}{\partial x^2} \quad (39)$$

$$AV_{0b} = \frac{C_{22}^b h_b}{R_b} w_{0b} + \frac{C_{23}^b h_b}{R_b}\frac{\partial u_{0b}}{\partial \theta} + \frac{C_{22}^b h_b}{R_b}\left(1 + \frac{h_b^2}{12R_b^2}\right)\frac{\partial v_{0b}}{\partial \theta} - \frac{C_{22}^b h_b^3}{12R_b^3}\frac{\partial^2 w_{0b}}{\partial \theta^2} + C_{12}^b h_b \frac{\partial u_{0b}}{\partial x} + C_{23}^b h_b \left(1 + \frac{h_b^2}{12R_b^2}\right)\frac{\partial v_{0b}}{\partial x} - \frac{C_{23}^b h_b^3}{6R_b^2}\frac{\partial^2 w_{0b}}{\partial x \partial \theta} - \frac{C_{12}^b h_b^3}{12R_b}\frac{\partial^2 w_{0b}}{\partial x^2} \quad (40)$$

$$AW_{0t} = \frac{C_{22}^t h_t^3}{12R_t^3}\frac{\partial^2 v_{0t}}{\partial \theta^2} - \frac{C_{22}^t h_t^3}{12R_t^3}\frac{\partial^3 w_{0t}}{\partial \theta^3} + \frac{C_{23}^t h_t^3}{4R_t^2}\frac{\partial^2 v_{0t}}{\partial x \partial \theta} - \frac{C_{23}^t h_t^3}{3R_t^2}\frac{\partial^3 w_{0t}}{\partial x \partial \theta^2} + \frac{C_{33}^t h_t^3}{6R_t}\frac{\partial^2 v_{0t}}{\partial x^2} - \frac{h_t^3}{12R_t}\left(C_{12}^t + 4C_{33}^t\right) \times \frac{\partial^3 w_{0t}}{\partial x^2 \partial \theta} - \frac{C_{13}^t h_t^3}{6}\frac{\partial^3 w_{0t}}{\partial x^3} + \frac{h_t R_c^2}{2R_t R_{tc}} T_{\theta z}^c(x,\theta) \quad (41)$$

$$AW_{0b} = \frac{C_{22}^b h_b^3}{12R_b^3}\frac{\partial^2 v_{0b}}{\partial \theta^2} - \frac{C_{22}^b h_b^3}{12R_b^3}\frac{\partial^3 w_{0b}}{\partial \theta^3} + \frac{C_{23}^b h_b^3}{4R_b^2}\frac{\partial^2 v_{0b}}{\partial x \partial \theta} - \frac{C_{23}^b h_b^3}{3R_b^2}\frac{\partial^3 w_{0b}}{\partial x \partial \theta^2} + \frac{C_{33}^b h_b^3}{6R_b}\frac{\partial^2 v_{0b}}{\partial x^2} - \frac{h_b^3}{12R_b}\left(C_{12}^b + 4C_{33}^b\right) \times \frac{\partial^3 w_{0b}}{\partial x^2 \partial \theta} - \frac{C_{13}^b h_b^3}{6}\frac{\partial^3 w_{0b}}{\partial x^3} + \frac{h_b R_c^2}{2R_b R_{bc}} T_{\theta z}^c(x,\theta) \quad (42)$$

$$ADW_{0t} = -\frac{C_{22}^t h_t^3}{12R_t^3}\frac{\partial v_{0t}}{\partial \theta} + \frac{C_{22}^t h_t^3}{12R_t^3}\frac{\partial^2 w_{0t}}{\partial \theta^2} - \frac{C_{23}^t h_t^3}{12R_t^2}\frac{\partial v_{0t}}{\partial x} + \frac{C_{23}^t h_t^3}{6R_t^2}\frac{\partial^2 w_{0t}}{\partial x \partial \theta} + \frac{C_{12}^t h_t^3}{12R_t}\frac{\partial^2 w_{0t}}{\partial x^2} \quad (43)$$

$$ADW_{0b} = -\frac{C_{22}^b h_b^3}{12R_b^3}\frac{\partial v_{0b}}{\partial \theta} + \frac{C_{22}^b h_b^3}{12R_b^3}\frac{\partial^2 w_{0b}}{\partial \theta^2} - \frac{C_{23}^b h_b^3}{12R_b^2}\frac{\partial v_{0b}}{\partial x} + \frac{C_{23}^b h_b^3}{6R_b^2}\frac{\partial^2 w_{0b}}{\partial x \partial \theta} + \frac{C_{12}^b h_b^3}{12R_b}\frac{\partial^2 w_{0b}}{\partial x^2} \quad (44)$$

Note that for considered boundary conditions the relations are as follows:

Clamped (C): $\delta u_{0t} = \delta u_{0b} = \delta v_{0t} = \delta v_{0b} = \delta w_{0t} = \delta w_{0b} = \delta \frac{\partial w_{0t}}{\partial \theta} = \delta \frac{\partial w_{0b}}{\partial \theta} = 0$.

Simply supported (S): $\delta u_{0t} = \delta u_{0b} = AV_{0t} = AV_{0b} = \delta w_{0t} = \delta w_{0b} = ADW_{0t} = ADW_{0b} = 0$

Free (F): $AU_{0t} = AU_{0b} = AV_{0t} = AV_{0b} = AW_{0t} = AW_{0b} = ADW_{0t} = ADW_{0b} = 0$.

Appendix B

Boundary conditions, on $x = 0, L$.

$$\delta u_{0t} BU_{0t} = 0 \quad (45)$$

$$\delta u_{0b} BU_{0b} = 0 \quad (46)$$

$$\delta v_{0t} BV_{0t} = 0 \quad (47)$$

$$\delta v_{0b} BV_{0b} = 0 \quad (48)$$

$$\delta w_{0t} BW_{0t} = 0 \quad (49)$$

$$\delta w_{0b} BW_{0b} = 0 \quad (50)$$

$$\delta \frac{\partial w_{0t}}{\partial x} BDW_{0t} = 0 \quad (51)$$

$$\delta \frac{\partial w_{0b}}{\partial x} BDW_{0b} = 0 \quad (52)$$

where.

$$BU_{0t} = C_{12}^t h_t w_{0t} + C_{13}^t h_t \frac{\partial u_{0t}}{\partial \theta} + C_{12}^t h_t \frac{\partial v_{0t}}{\partial \theta} + C_{11}^t h_t R_t \frac{\partial u_{0t}}{\partial x} + C_{13}^t h_t R_t \frac{\partial v_{0t}}{\partial x} \quad (53)$$

$$BU_{0b} = C_{12}^b h_b w_{0b} + C_{13}^b h_b \frac{\partial u_{0b}}{\partial \theta} + C_{12}^b h_b \frac{\partial v_{0b}}{\partial \theta} + C_{11}^b h_b R_b \frac{\partial u_{0b}}{\partial x} + C_{13}^b h_b R_b \frac{\partial v_{0b}}{\partial x} \quad (54)$$

$$BV_{0t} = C_{23}^t h_t w_{0t} + C_{33}^t h_t \frac{\partial u_{0t}}{\partial \theta} + C_{23}^t h_t \left(1 + \frac{h_t^2}{12R_t^2}\right)\frac{\partial v_{0t}}{\partial \theta} - \frac{C_{23}^t h_t^3}{12R_t^2}\frac{\partial^2 w_{0t}}{\partial \theta^2} + C_{13}^t h_t R_t \frac{\partial u_{0t}}{\partial x} + C_{33}^t h_t \left(R_t + \frac{h_t^2}{12R_t}\right) \times \frac{\partial v_{0t}}{\partial x} - \frac{C_{33}^t h_t^3}{6R_t}\frac{\partial^2 w_{0t}}{\partial x \partial \theta} - \frac{C_{13}^t h_t^3}{12}\frac{\partial^2 w_{0t}}{\partial x^2} \quad (55)$$

$$BV_{0b} = C_{23}^b h_b w_{0b} + C_{33}^b h_b \frac{\partial u_{0b}}{\partial \theta} + \left(\frac{C_{23}^b h_b^3}{12R_b^2} + C_{23}^b h_b\right)\frac{\partial v_{0b}}{\partial \theta} - \frac{C_{23}^b h_b^3}{12R_b^2}\frac{\partial^2 w_{0b}}{\partial \theta^2} + C_{13}^b h_b R_b \frac{\partial u_{0b}}{\partial x} + \left(C_{33}^b h_b R_b + \frac{C_{33}^b h_b^3}{12R_b}\right) \frac{\partial v_{0b}}{\partial x} - \frac{C_{33}^b h_b^3}{6R_b}\frac{\partial^2 w_{0b}}{\partial x \partial \theta} - \frac{C_{13}^b h_b^3}{12}\frac{\partial^2 w_{0b}}{\partial x^2} \quad (56)$$

$$BW_{0t} = \frac{C_{23}^t h_t^3}{6R_t^2}\frac{\partial^2 v_{0t}}{\partial\theta^2} - \frac{C_{23}^t h_t^3}{6R_t^2}\frac{\partial^3 w_{0t}}{\partial\theta^3} + \left(\frac{C_{12}^t h_t^3}{12R_t} + \frac{C_{33}^t h_t^3}{6R_t}\right)\frac{\partial^2 v_{0t}}{\partial x\partial\theta} - \left(\frac{C_{12}^t h_t^3}{12R_t} + \frac{C_{33}^t h_t^3}{3R_t}\right)\frac{\partial^3 w_{0t}}{\partial x\partial\theta^2} + \frac{C_{13}^t h_t^3}{12}\frac{\partial^2 v_{0t}}{\partial x^2} - \frac{C_{13}^t h_t^3}{3}\frac{\partial^3 w_{0t}}{\partial x^2\partial\theta} - \frac{C_{11}^t h_t^3 R_t}{12}\frac{\partial^3 w_{0t}}{\partial x^3} + \frac{h_t R_c}{2}T_{xz}^c(x,\theta) \tag{57}$$

$$BW_{0b} = \frac{C_{23}^b h_b^3}{6R_b^2}\frac{\partial^2 v_{0b}}{\partial\theta^2} - \frac{C_{23}^b h_b^3}{6R_b^2}\frac{\partial^3 w_{0b}}{\partial\theta^3} + \left(\frac{C_{12}^b h_b^3}{12R_b} + \frac{C_{33}^b h_b^3}{6R_b}\right)\frac{\partial^2 v_{0b}}{\partial x\partial\theta} - \left(\frac{C_{12}^b h_b^3}{12R_b} + \frac{C_{33}^b h_b^3}{3R_b}\right)\frac{\partial^3 w_{0b}}{\partial x\partial\theta^2} + \frac{C_{13}^b h_b^3}{12}\frac{\partial^2 v_{0b}}{\partial x^2} - \frac{C_{13}^b h_b^3}{3}\frac{\partial^3 w_{0b}}{\partial x^2\partial\theta} - \frac{C_{11}^b h_b^3 R_b}{12}\frac{\partial^3 w_{0b}}{\partial x^3} + \frac{h_b R_c}{2}T_{xz}^c(x,\theta) \tag{58}$$

$$BDW_{0t} = -\frac{C_{12}^t h_t^3}{12R_t}\frac{\partial v_{0t}}{\partial\theta} + \frac{C_{12}^t h_t^3}{12R_t}\frac{\partial^2 w_{0t}}{\partial\theta^2} - \frac{C_{13}^t h_t^3}{12}\frac{\partial v_{0t}}{\partial x} + \frac{C_{13}^t h_t^3}{6}\frac{\partial^2 w_{0t}}{\partial x\partial\theta} + \frac{C_{11}^t h_t^3 R_t}{12}\frac{\partial^2 w_{0t}}{\partial x^2} \tag{59}$$

$$BDW_{0b} = -\frac{C_{12}^b h_b^3}{12R_b}\frac{\partial v_{0b}}{\partial\theta} + \frac{C_{12}^b h_b^3}{12R_b}\frac{\partial^2 w_{0b}}{\partial\theta^2} - \frac{C_{13}^b h_b^3}{12}\frac{\partial v_{0b}}{\partial x} + \frac{C_{13}^b h_b^3}{6}\frac{\partial^2 w_{0b}}{\partial x\partial\theta} + \frac{C_{11}^b h_b^3 R_b}{12}\frac{\partial^2 w_{0b}}{\partial x^2} \tag{60}$$

Note that, for considered boundary conditions, the relations are as follows:

Clamped (C): $\delta u_{0t} = \delta u_{0b} = \delta v_{0t} = \delta v_{0b} = \delta w_{0t} = \delta w_{0b} = \delta\frac{\partial w_{0t}}{\partial x} = \delta\frac{\partial w_{0b}}{\partial x} = 0$.

Simply supported (S):$\delta u_{0t} = \delta u_{0b} = BV_{0t} = BV_{0b} = \delta w_{0t} = \delta w_{0b} = BDW_{0t} = BDW_{0b} = 0$

Free (F): $BU_{0t} = BU_{0b} = BV_{0t} = BV_{0b} = BW_{0t} = BW_{0b} = BDW_{0t} = BDW_{0b} = 0$.

References

1. Plantema FJ (1966) Sandwich construction. Wiley, New York
2. Allen HG (1969) Analysis and design of structural sandwich panels. Pergamon Press Inc, Oxford
3. Zenkert D (1995) An introduction to sandwich construction. Chameleon Press, London
4. Noor AK, Burton WS, Bert CW (1996) Computational models for sandwich panels and shells. Appl Mech Rev 49:155–199
5. Librescu L, Hause T (2000) Recent developments in the modeling and behavior of advanced sandwich constructions: a survey. Compos Struct 48:1–17
6. Vinson JR (2001) Sandwich structures. Appl Mech Rev 54:201–214
7. Altenbach H (2011) Mechanics of advanced materials for lightweight structures. Proc ImechE Part C J Mech Eng Sci 225:2481–2496
8. Frostig Y, Baruch M, Vilnay O, Sheinman I (1992) High-order theory for sandwich-beam behavior with transversely flexible core. J Eng Mech 118:1026–1043
9. Frostig Y, Baruch M (1996) Localized load effects in high-order bending of sandwich panels with transversely flexible core. J Eng Mech 122:1069–1076
10. Thomsen OT, Frostig Y (1997) Localized bending effects in sandwich panels: photoelastic investigation vs high-order sandwich theory results. Compos Struct 37:97–108
11. Frostig Y (1999) Bending of curved sandwich panels with transversely flexible core-closed form high-order theory. J Sand Struct Mater 1:4–41
12. Li R, Frostig Y, Kardomateas GA (2001) Nonlinear high-order response of imperfect sandwich beams with delaminated faces. AIAA J 39:1782–1787
13. Li R, Kardomateas GA (2009) A high-order theory for cylindrical sandwich shells with flexible cores. J Mech Mater Struct 4:1453–1467
14. Afshin M, Sadighi M, Shakeri M (2010) Static analysis of cylindrical sandwich panels with a flexible core and laminated composite face sheets. J Compos Mater 44:1455–1476
15. Rahmani O, Khalili SMR, Thomsen OT (2012) A high-order theory for the analysis of circular cylindrical composite sandwich shells with transversely compliant core subjected to external loads. Compos Struct 94:2129–2142
16. Carrera E, Brischetto S (2009) A comparison of various kinematic models for sandwich shell panels with soft core. J Compos Mater 43:2201–2221
17. Civalek Ö (2004) Application of differential quadrature (DQ) and harmonic differential quadrature (HDQ) for buckling analysis of thin isotropic plates and elastic columns. Eng Struct 26:171–186
18. Shu C (2000) Differential quadrature and its application in engineering. Springer, Berlin
19. Shu C, Richards BE (1992) Application of generalized differential quadrature to solve two-dimensional incompressible Navier Stockes equations. Int J Numer Methods Fluids 15:791–798
20. Bellman R, Kashef BG, Casti J (1972) Differential quadrature: a technique for the rapid solution of nonlinear partial differential equations. J Comput Phys 10:4–52
21. Maleki S, Tahani M, Andakhshideh A (2012) Static and transient analysis of laminated cylindrical shell panels with various boundary conditions and general lay-ups. ZAMM Z Angew Math Mech 92:124–140
22. Tornabene F, Liverani A, Caligiana G (2012) Static analysis of laminated composite curved shells and panels of revolution with a posteriori shear and normal stress recovery using generalized differential quadrature method. Int J Mech Sci 61:71–87
23. Malekzadeh P (2009) A two-dimensional layerwise-differential quadrature static analysis of thick laminated composite circular arches. Appl Math Model 33:1850–1861
24. Reddy JN (2003) Mechanics of laminated composite plates and shells: theory and analysis. CRC Press, Florida
25. Soedel W (2004) Vibrations of shells and plates. Marcel Dekker Inc, New York
26. Washizu K (1975) Variational methods in elasticity and plasticity. Pergamon Press, Oxford
27. Rao T (2002) Study of core compression using digital image correlation (DIC). Master of Science Dissertation, Michigan Technological University